Journal of Antimicrobial Chemotherapy (2008) **61**, 95–102
doi:10.1093/jac/dkm400
Advance Access publication 24 October 2007

JAC

Evaluation of Fourier transform infrared spectroscopy for the rapid identification of glycopeptide-intermediate *Staphylococcus aureus*

Nassim M. Amiali[1,2]*, Michael R. Mulvey[3], Brigitte Berger-Bächi[4], Jacqueline Sedman[2], Andrew E. Simor[5] and Ashraf A. Ismail[2]

[1]Quelab Laboratories Inc., Montreal, QC, Canada; [2]McGill IR Group, McGill University, Montreal, QC, Canada; [3]Nosocomial Infections, National Microbiology Laboratory, Public Health Agency of Canada, Winnipeg, MB, Canada; [4]Institute of Medical Microbiology, University of Zürich, Switzerland; [5]Sunnybrook and Women's College, Health Science Center, Toronto, ON, Canada

Received 9 July 2007; returned 8 August 2007; revised 21 September 2007; accepted 26 September 2007

***Objectives*: To evaluate Fourier transform infrared (FTIR) spectroscopy as a rapid method for distinguishing glycopeptide-intermediate *Staphylococcus aureus* (GISA) from glycopeptide-susceptible methicillin-resistant *S. aureus* (MRSA) and to compare three data analysis methods.**

***Methods*: First-derivative normalized spectra of dried films of bacterial growth on Que-Bact® Universal Medium No. 2 were examined by singular value decomposition to identify key spectral regions. Region selection was analysed by principal component analysis (PCA), self-organizing maps (SOMs) and the *K*-nearest neighbour (KNN) algorithm. The initial data set included 35 GISA (including GISA Mu50 and heterogeneous GISA Mu3) and 25 epidemic MRSA. The regions were then tested using enlarged data sets that included 22 sporadic and 85 additional epidemic MRSA.**

***Results*: Epidemic MRSA and GISA/hGISA were separated into two distinct clusters on the basis of spectral data from regions 1352–1315 and 1480–1460 cm^{-1}, the former providing 100% correct classification by all three analyses and the latter providing 96.67% correct by PCA, 98.34% by SOM and 100% by KNN. The 1480–1460 cm^{-1} region was more effective for distinguishing GISA/hGISA from a set combining sporadic and epidemic MRSA, with two GISA/hGISA and four sporadic MRSA misclassified by PCA and SOM (92.69% correct), while the KNN method misclassified three of the four sporadic MRSA (93.90% correct). The addition of 85 other epidemic MRSA this set increased the fraction of correctly classified isolates to 96.41% and 97.01% by PCA, SOM and KNN, respectively.**

***Conclusions*: As only 6 of 167 isolates were misclassified, FTIR spectroscopy may provide means of rapid and accurate identification of GISA and hGISA among isolates of MRSA.**

Keywords: infrared spectroscopic method, glycopeptide resistance, heterogeneous GISA, MRSA

Introduction

Methicillin-resistant *Staphylococcus aureus* (MRSA) is one of the most common agents of community-acquired and nosocomial infections worldwide, causing high morbidity and mortality. For the past three decades, glycopeptides have been the antibiotics of choice for the treatment of MRSA infections. In recent years, however, MRSA with varying degrees of reduced susceptibility to glycopeptides have emerged, the so-called 'glycopeptide-intermediate' strains or GISA. These are characterized by MICs of 8–16 mg/L for teicoplanin and ≥8 mg/L for vancomycin. This situation is complicated by heterogeneous forms called hGISA, with MICs of 16 mg/L for teicoplanin and 1–4 mg/L for vancomycin. These appear to give rise to subpopulations able to grow in the presence of over 4 mg/L of vancomycin at a frequency of 10^{-6} or higher[1–4] and may underlie some failures of vancomycin therapy.[5–7] However, the true clinical incidence and significance of hGISA remain unclear.

The mechanism of glycopeptide resistance has not been fully defined and clinical detection continues to rely on growth and susceptibility in selective media, often giving ambiguous results.[1,5,8,9] Thus there is a need in clinics for a more reliable

*Corresponding author. Tel: +1-514-277-2558, ext. 13; Fax: +1-514-277-4714; E-mail: nassim.amiali@gmail.com

method of screening MRSA for the glycopeptide resistance trait. Such a method should be simple and rapid and offer high reproducibility both within and between laboratories.

The GISA/hGISA phenotype may be confirmed by population analysis[1] and/or by electron microscopy (thickened cell wall), both too complex and costly for routine clinical practice. The gold standard method, used in a number of surveillance studies for GISA and hGISA, is the population analysis profile (PAP)-area under the curve (AUC),[10–12] with criteria specifically designed to discriminate between glycopeptide-susceptible *S. aureus*, hGISA and GISA. Ideally, PAP-AUC would be used in clinics to confirm the GISA/hGISA phenotypes when identified by a reliable and preferably rapid screening method.

Several screening methods and agars for GISA/hGISA have been reported.[1,13,14] In a recent international study involving 12 laboratories,[15] the macro-method Etest (MET) and Mueller–Hinton agar (MHA) with 5 mg/L teicoplanin provided correct identification of 82.5% and 85.9% of 48 test strains, whereas brain–heart infusion agar (BHIA) broth with 6 mg/L vancomycin identified only 11.5% of the hGISA in the set and gave the highest inter-laboratory variability for GISA in general.

The GISA phenotype is associated with alterations in the cell-wall peptidoglycan synthesis pathway and increased levels of penicillin-binding proteins (PBP2), resulting in thickened cell walls.[16] Biochemical characteristics such as these are detectable by Fourier transform infrared (FTIR) spectroscopy, a non-destructive technique that can be used to probe the total composition of intact microbial cells without the use of reagents. Complex yet distinct and reproducible spectral signatures or 'fingerprints' of microorganisms may be obtained for identification purposes, even down to the subspecies[17–22] and antibiotic resistance phenotypes.[23–25] On the basis of these findings, the present study was undertaken to evaluate its potential as a superior alternative to conventional clinical screening methods for distinguishing the GISA/hGISA phenotype from glycopeptide-susceptible *S. aureus*.

Materials and methods

Clinical specimens and microbiological analysis

The 35 GISA/hGISA isolates were obtained from the Network on Antimicrobial Resistance in *S. aureus* (NARSA) collection. These included 31 methicillin-resistant and 4 methicillin-susceptible GISA/hGISA isolates. Heterogeneous GISA strain Mu3 and GISA strain Mu50 were included among the 31 methicillin-resistant GISA/hGISA. Eighty-five isolates of epidemic MRSA and 22 isolates of sporadic MRSA were provided by the Health Canada National Microbiology Laboratory (NML). Another 25 epidemic MRSA were provided by the Royal Victoria Hospital (Montreal, QC, Canada).

Testing for glycopeptide-intermediate resistance in all GISA/hGISA was performed by NARSA using broth microdilution (BMD) with frozen and dried panels; conventional MET with MHA, 0.5 McFarland inoculum and 24 h incubation at 35°C (MHA-CMET); the modified MET with BHIA, 2.0 McFarland inoculum and 48 h incubation at 35°C (BHIA-MMET); the BHIA screen assay (24, 48 and 72 h growth of 10 μL spot on agar containing 6 mg/L vancomycin or BHIA-6V); and the conventional disc diffusion method (DD). In fact, identification of an isolate as GISA or hGISA by NARSA is based solely on the BHIA-MMET method.

FTIR spectroscopic methods

Sample preparation. All isolates were grown from frozen stocks kept at −70°C in BHI broth containing 15% glycerol, by overnight subculture on tryptic soy agar with sheep blood (Quelab Laboratories Inc., Montreal, QC, Canada) at 37°C. A single colony was collected, streaked in a four-quadrant pattern onto four plates of Que-Bact® Universal Medium No. 2 agar (Quelab Laboratories Inc.), which were then incubated for 18 h at 37°C. Cells were then carefully collected from a single quadrant of each plate using a 10 mm diameter soft plastic loop (10 μL, COP-S10, Copan Diagnostics Inc., Corona, CA, USA). All surfaces of the loop head are ultra-smooth for easy streaking or harvesting of growth, without damaging or scraping the agar surface. Collected colonies were suspended in the same 200 μL aliquot of sterile physiological saline (0.9% NaCl), which was then diluted 10-fold in saline to a cell concentration of $\sim 5 \times 10^{11}$ cfu/mL. A 25 μL droplet of diluted suspension was deposited on a clean zinc selenide (ZnSe) optical window (13 mm diameter, 2 mm thick, two windows per aluminium slide) and oven-dried at 48°C for 1 h to form a thin and transparent homogeneous dried film for FTIR measurement. Four films were made for each isolate.

Spectral acquisition. All FTIR spectra were acquired in the transmission mode using a Bomem MB-104 (ABB-Bomem, Quebec, QC, Canada) FTIR spectrometer equipped with a non-hygroscopic ZnSe beamsplitter and a deuterated triglycine sulphate detector and operating under Bomem-Grams/386 software (Galactic, Salem, NH, USA). The spectrometer was purged with dry CO_2-free air from a Balston dryer (Balston, Lexington, MA, USA) to minimize interference from atmospheric water vapour and CO_2. To enhance the signal-to-noise ratio, 64 scans were co-added at 4 cm^{-1} resolution over the wavenumber range of 4000–400 cm^{-1} and ratioed against an open-beam background to obtain an absorbance spectrum. A single spectrum was thus obtained for each of the four windows made for each strain.

Tentative assignments of spectral features based on the comparison of resolution-enhanced microbial IR spectra with IR spectra of known building blocks inherent in intact cells are described as follows.[26]

The spectral region of 3000–2800 cm^{-1} is dominated by broad features resulting from vibrations of $-CH_3$, $>CH_2$ and CH functional groups of fatty acid aliphatic chains. The region between 1800 and 1500 cm^{-1} contains bands corresponding to protein and peptide components such as amides I and II. The 1500–1200 cm^{-1} region is mixed and contains vibrations corresponding to carboxylic groups of proteins, free amino acids and polysaccharides as well as vibrations of phosphate, RNA/DNA and phospholipids. The 1200–900 cm^{-1} region is dominated by absorption bands corresponding to cell-wall carbohydrates. The 900–700 cm^{-1} region is yet to be associated with specific components.

Mathematical pre-processing and processing. Spectra acquired in Grams SPC format were converted into comma-separated value files and then into MATLAB files using MATLAB version 5.1 (The MathWorks, Inc., Natick, MA, USA). Because band intensity varies as a function of film thickness, the spectral data over the whole spectral range (4000–400 cm^{-1}) were normalized to unit height by vector transformation to compensate for differences in film thickness and then transformed to the first derivative using the Savitzky–Golay algorithm to maximize peak separation, enhance apparent resolution and minimize problems arising from baseline shifts.

Prior to data processing, spectral feature selection was performed by singular value decomposition (SVD)[27] using pairs of spectra and confirmed by visual examination of the normalized spectra. Data were processed using two exploratory data analysis methods, namely,

principal component analysis or PCA (employing the non-linear iterative partial-least-squares algorithm[28]) and the self-organizing map (SOM) algorithm.[29] Cluster analysis was performed using the *K*-nearest neighbours (KNN) algorithm.[30] Programs were written in MATLAB version 5.1 to implement the data pre-processing and processing algorithms.

SVD algorithm. Spectral regions having features with the potential to distinguish all the strains were pre-selected using the SVD algorithm.[27] The SVD algorithm inspects IR spectral region vectors (columns of matrix U and absorbance at specific wavenumbers) corresponding to the most significant features and compares each vector to a threshold value. If the threshold is exceeded, the corresponding spectral region is assigned to the clustering set.

Principal component analysis. PCA is a multivariate procedure that rotates data to maximize the variability projected onto axes. A set of correlated variables is thus transformed to a set of uncorrelated variables ranked by variability in the descending order.[28] The resulting uncorrelated variables are linear combinations of the original variables and the last of these can be removed with minimal loss of real data. PCA is used mainly to reduce the dimensionality of a data set while retaining as much information as possible by computing a compact and optimal description of the data set. The first principal component (PC1) is the combination of variables that accounts for the greatest amount of the total variation. The second principal component (PC2) defines the largest amount of the remaining variation and is orthogonal to the first principal component. The number of principal components possible is equal to the number of variables. In addition to reducing the number of variables and detecting structural relationship between variables, a PCA plot shows spectral data distribution and hence the existence of clusters.

Self-organizing maps. SOM is a data visualization technique that uses unsupervised self-organizing neural networks to reduce the dimensionality of data to a level that humans can comprehend.[29] This usually means producing a one- or two-dimensional map that plots similarities by grouping similar data items together. The map consists of a regular grid of processing units or 'neurons'. Each neuron k is represented by an n-dimensional prototype vector $m_k = [m_{k1},\ldots, m_{kn}]$ where n is the dimension of the input space. At each training step, a data sample x is selected and the nearest neuron m_c [referred to as the best matching unit (BMU)] is found. The prototype vectors of the BMU and its neighbours on the grid are moved towards the sample vector according to the relation:

$$m_k := m_k + \alpha(t)h_{ck}(t)(x - m_k)$$

where $\alpha(t)$ is the learning rate and $h_{ck}(t)$ is a neighbourhood kernel centred on the BMU. Both learning rate and neighbourhood kernel radius decease monotonically with time. During iterative training of the network, a multidimensional model emerges, containing all the spectral features associated with each prototype vector. The map attempts to represent all the available observations with optimal accuracy using a restricted set of models (neurons) of meaningful two-dimensional order. At the same time, models or neurons become ordered on the grid according to their similarity to each other, resulting in a clustering diagram.[29]

K-nearest neighbour. The KNN classifier is a non-parametric similarity classification-based method that attempts to categorize unknown samples based on multivariate proximity to other samples of pre-assigned categories. The distance matrix is sorted and the distance of the unknown sample is compared with its KNNs. The identity of an unknown sample is based on the class of the nearest known samples, that is, by assigning the class shared by the majority of nearest neighbours to the unknown. Each class represents a bacterial strain type in the data set. The optimal number K of neighbours used to predict an unknown was determined from the highest number of correctly classified points obtained with K set at 1 through 10.[30]

Results and discussion

The emergence of *S. aureus* in many parts of the world with decreased susceptibility to glycopeptide antimicrobial agents such as vancomycin and teicoplanin is a major concern.[9] It is particularly worrisome that hetero-resistant strains (hGISA) appear susceptible based on the conventional testing, but give rise to more resistant forms at a frequency of about one cell per million. Both GISA and hGISA confound routine methods used in diagnostic laboratories. The use of BHI agar with 6 mg/L vancomycin (BHIA-6V) or of Mueller–Hinton agar with 5 mg/L teicoplanin and the MET appears to be $<86\%$ accurate and with considerable inter-laboratory variability.[15] The true clinical incidence of GISA and in particular hGISA will not be known until a reliable detection method is available at a cost affordable by diagnostic laboratories. Such a method must minimize false-positive results, as it would be highly desirable to do the expensive confirmatory tests (PAP-AUC) when screening results are positive. Diagnostic laboratories will therefore assess the performance of any GISA/hGISA screening method in terms of cost-effectiveness. Reproducibility and variability of performance between laboratories is of concern, especially for public health and research. FTIR spectroscopy has the potential to offer a method that is affordable and reproducible both within and between laboratories.

Spectral reproducibility

The fundamental requirement for IR analysis of microorganisms is that the variance among spectra of a single taxon be less than that among spectra of different taxa.[31] In this context, it should be emphasized that IR spectroscopy is sensitive to phenotypic rather than genotypic differences; that is, it measures the biochemical expression of genes under a specific set of conditions rather than the presence of specific genes. As variations in biochemical composition among different taxa may be slight, spectral reproducibility depends on stringent control of sampling and measurement conditions. The composition of the growth medium and phase of growth (stationary versus exponential) are critical, as relative peak intensities may be affected much more (because of changes in metabolite pools) than peak positions.[32] FTIR analysis thus depends very much on fidelity in the reproduction of growth media, culture handling techniques and culture conditions.[31,33,34] An 'IR grade' standard blood-free synthetic growth medium, namely Que-Bact® Universal Medium No. 2 developed by Quelab Laboratories Inc., and strict observance of 18 h incubations at 37°C to obtain early stationary-phase cells on a consistent basis were employed in the present study.

There is a theoretical possibility of variance due to carry-over (from the medium used to reactivate the frozen strains) of sheep blood from different sources. Three years of practice have indicated that this does have any appreciable impact on spectral

consistency (data not shown). It is also important to collect colonies uncontaminated by agar. This is ensured using a large plastic loop that gathers a large amount of bacterial growth without scraping the agar surface. The exact manner in which different individuals collect the growth and produce the cell suspension could introduce variance, but no spectral variations were attributable to this factor.

For spectra acquired in the transmission mode, reproducibility is affected by sample uniformity, in particular homogeneity, particle size and thickness or light path length.[35] Drying a 25 μL droplet of diluted bacterial suspension for 1 h at 48°C yielded a transparent and uniform film and avoided baseline variations as well as scattering, diffraction and refraction of the infrared beam. Variations in the sample thickness cause band intensity to vary, although relative peak intensities may be maintained. Comparison of the spectra between 1800 and 800 cm^{-1} of the four films prepared for each isolate (from a suspension of colonies from four separate plates) yielded an average correlation coefficient of $r = 0.97$ (data not shown). Variations were further minimized by normalization to unit peak height and transformation to the first derivative, which highlights spectral shapes and contours and removes the effects of baseline shift, assuming that the spectra possess a sufficient signal-to-noise ratio. Finally, the use of a highly hygroscopic FTIR spectrometer equipped with a ZnSe beamsplitter improves reproducibility for long-term intra- and inter-laboratory comparisons.

Spectral differences between MRSA and GISA/hGISA

Infrared spectra of microorganisms have extensive overlap because of bio-molecules common to all cells, and the subtle differences among strains may be difficult to detect. The differentiation of GISA/hGISA and MRSA on the basis of their FTIR spectra may be categorized as a pattern recognition task. As in any such task, feature extraction using the SVD algorithm may assist in the selection of spectral regions for identification purposes. A random selection among the 240 spectra obtained for the 35 GISA/hGISA and 25 NML epidemic MRSA isolates allowed us to identify two narrow regions with clear differences using SVD: (i) 1480–1460 cm^{-1} (Figure 1), assignable to deformation vibrations of C-H bonds in methylene (CH_2) groups of lipids and proteins; and (ii) 1352–1315 cm^{-1} (Figure 2), attributable to symmetric stretching vibrations of carboxyl groups of amino acid side chains or free fatty acids.

Discrimination between MRSA and GISA/hGISA based on the 1480–1460 cm^{-1} region

The first three principal components (PC1, PC2 and PC3) accounted for over 99.94% of the total variance, with PC1 and PC2 alone accounting for 97.92% and 1.84%, respectively. The PCA scores plot (PC1 versus PC2) gave two distinct clusters, corresponding to MRSA and GISA/hGISA (Figure 3). Two GISA/hGISA isolates, NRS4 and NRS68, were misclassified as MRSA, yielding an overall correct classification of 96.67%. Visual inspection of an SOM of size [14 × 6] generated by nonlinear projection of the PC1 and PC2 scores and trained using a rough training phase of 4 iterations and a fine-tuning phase of 14 epochs also indicated two distinct clusters corresponding to MRSA and GISA/hGISA (Figure 4). The learning rate decreased

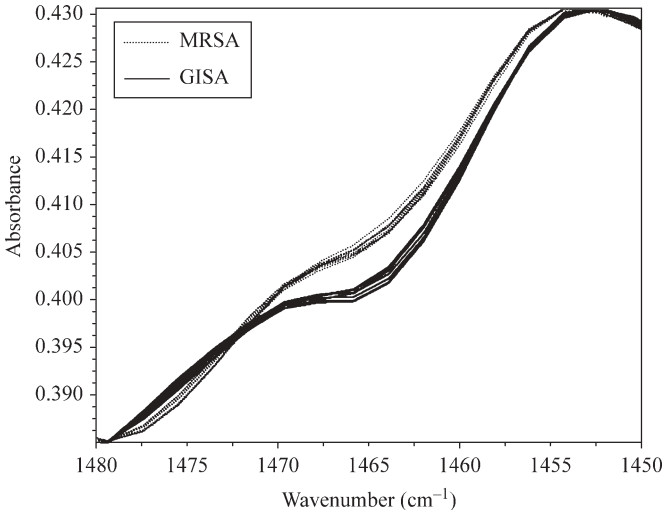

Figure 1. FTIR spectra of GISA/hGISA (solid lines) and MRSA (dotted lines) in the region 1480–1450 cm^{-1}. A colour version of this figure is available as Supplementary data at *JAC* Online (http://jac.oxfordjournals.org/).

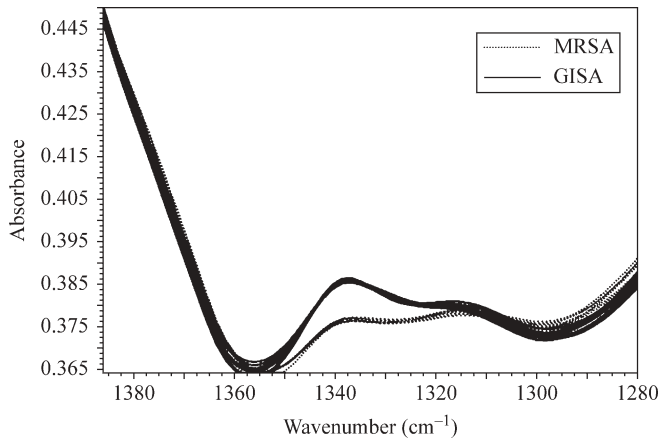

Figure 2. FTIR spectra of GISA/hGISA (solid lines) and MRSA (dotted lines) in the region 1380–1280 cm^{-1}. A colour version of this figure is available as Supplementary data at *JAC* Online (http://jac.oxfordjournals.org/).

linearly to zero during the fine-tuning phase with a final quantization error of 0.162 and a final topographic error of 0.048, yielding an overall correct classification of 98.34% with a single misclassified GISA/hGISA isolate, NRS68. This misclassified isolate cannot be visualized, as only the BMUs are shown. None of the four NRS68 replicates were classified as a BMU and therefore could be visualized only when plotting all data neighbours and BMUs at the same time, which would make the map difficult to visualize because of the large number of data. The supervised cluster analysis using the KNN algorithm with 120 spectra as the training set and the remaining 120 spectra as the test set gave 100% correct classification with $K = 1$ and $K = 2$.

Discrimination between MRSA and GISA/hGISA based on the 1352–1315 cm^{-1} region

Using the region 1352–1315 cm^{-1}, clustering of epidemic MRSA and GISA/hGISA was 100% correct by PCA, SOM and

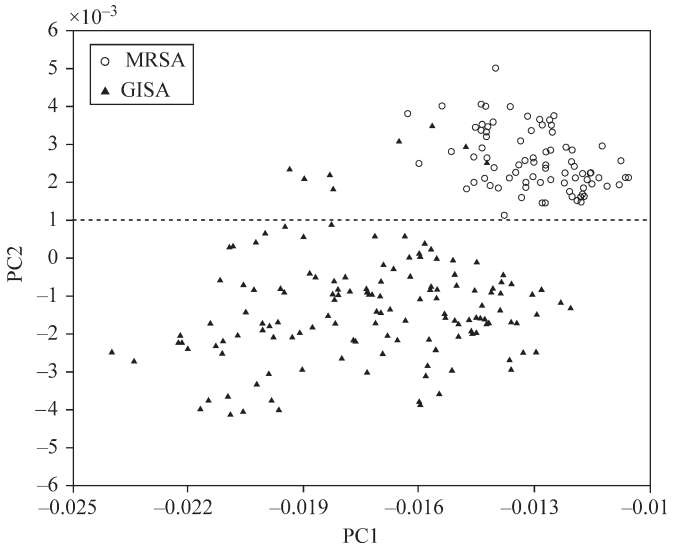

Figure 3. Scores plot for the first two principal components obtained from FTIR spectra of GISA/hGISA (filled triangles) and MRSA (open circles) in the region 1480–1460 cm^{-1}. A colour version of this figure is available as Supplementary data at *JAC* Online (http://jac.oxfordjournals.org/).

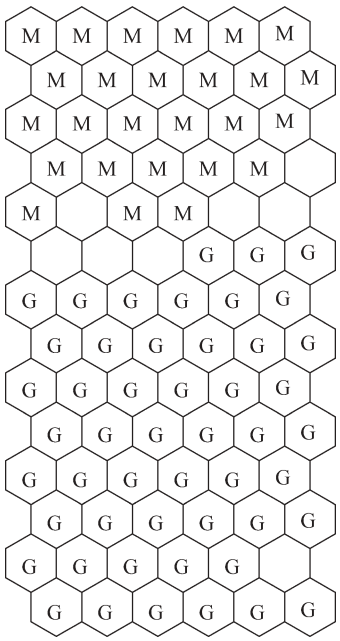

Figure 4. SOM obtained using FTIR spectral profiles of GISA/hGISA (G) and MRSA (M) in the region 1480–1460 cm^{-1}. A colour version of this figure is available as Supplementary data at *JAC* Online (http://jac.oxfordjournals.org/).

KNN. Two distinct clusters of GISA/hGISA and epidemic MRSA were clearly visible on the PCA plot and on an SOM of size [16 × 5] generated by non-linear projection of the PC1 and PC2 scores for this region using 4 iterations for rough training and 13 epochs for the fine-tuning phase (data not shown). The final quantization error was 0.128 with a final topological error of 0.008. Using half of the data set ($n = 120$) as the training set and the other half as the prediction set, the KNN algorithm was most effective for $K = 1$ and $K = 2$.

Discrimination between epidemic MRSA/sporadic MRSA and GISA/hGISA

Twenty-two sporadic MRSA isolates were added to investigate the ability of FTIR to distinguish GISA/hGISA from both sporadic and epidemic MRSA. The expanded data set contained four replicate spectra for each isolate for a total of 328 spectra. The region 1352–1315 cm^{-1}, although suitable for discriminating between epidemic MRSA and GISA/hGISA, proved unsuitable for discriminating between sporadic MRSA and GISA/hGISA, yielding an overall correct classification of only 84.15% by PCA, with 13 sporadic MRSA misclassified (data not shown). Some improvement was obtained using PCA with the region 1480–1460 cm^{-1}. The first three PCs contained over 99.9% of the overall total variance, with totals of 98.18%, 99.75% and 99.93% for PC1, PC2 and PC3, respectively, the scores plot of PC1 versus PC2 revealing two distinct clusters corresponding to GISA/hGISA and MRSA (data not shown). However, three sporadic MRSA isolates (715, 864 and 693) were misclassified as GISA/hGISA strains and a single sporadic MRSA (105) fell between the GISA/hGISA and MRSA cluster. The same two GISA/hGISA strains already mentioned (NRS4 and NRS68) fell within the MRSA cluster, yielding 92.69% overall correct classification. The SOM algorithm sorted the scores of PCs 1 and 2 into clear clusters of GISA/hGISA and MRSA (data not shown) with sporadic MRSA isolates 182, 715, 864 and 693 as well as GISA/hGISA isolates NRS4 and NRS68 misclassified, yielding 92.69% overall correct classification. The map of size [13 × 7] was trained using a short rough training phase of three iterations that corresponded to the first stage in which the initial order is formed. The initial weight vector, a large neighbourhood radius and a large learning rate were then applied and the remaining iteration stages constituted a fine-tuning phase of 11 epochs in which both learning rate and neighbourhood radius began at small values and were gradually reduced at each iteration. The learning rate decreased linearly to zero during the fine-tuning phase with a final quantization error of 0.173 and a final topographic error of 0.009. Supervised classification performed with the KNN algorithm using half of the data set ($n = 170$) as the training set and the other half as the prediction set gave a slightly higher correct classification of 93.9% using $K = 7$. The same three sporadic MRSA (715, 864 and 693) and the same two GISA/hGISA (NRS4 and NRS68) misclassified by the PCA scores plot were also misclassified by KNN. The single sporadic MRSA (105) that fell between the GISA/hGISA and MRSA clusters was correctly classified on the basis of the class of the majority of its nearest neighbouring known samples.

Validation of the FTIR method

The robustness of the differentiation using the 1480–1460 cm^{-1} region was assessed by challenging it with another collection of epidemic MRSA isolates. Sixty of these were collected by NML from various Canadian sources, whereas the other 25 were provided by a single hospital (Montreal Royal Victoria). Classification of a set containing these plus the original 35 GISA/hGISA strains was 98.34% correct by PCA with the same GISA/hGISA isolates as mentioned above misclassified (NRS4 and NRS68) and 99.37% correct by SOM and KNN for $K = 3$ with a single strain of GISA (NRS 68) misclassified. When these 85 epidemic MRSA were combined with the initial

expanded set of 82 isolates (i.e. including the sporadic MRSA), the same four sporadic MRSA (715, 693, 864 and 105) and two GISA/hGISA (NRS4 and NRS68) strains remained misclassified by PCA but the larger set increased the percent correct classification from 92.69% to 96.41%. For SOM, sporadic MRSA isolates 715, 693, 864 and 182 were again misclassified as well as GISA/hGISA isolates NRS4 and NRS68, thus increasing the correct classification from 92.69% to 96.41% as for PCA. Correct classification by the KNN analysis also increased, from 93.90% to 97.01% for $K = 7$, with the same three sporadic MRSA (715, 693 and 864) and the same GISA/hGISA (NRS4 and NRS68) misclassified.

Other work has shown that *Enterococcus casseliflavus* and *Enterococcus gallinarum* with intrinsic low-level vancomycin resistance were correctly identified by FTIR spectroscopy[18] using a combination of equally weighted broad spectral ranges (1500–1200, 1200–900, 900–700 cm^{-1}) of first-derivative spectra. However, these species were not distinguished from vancomycin-susceptible strains of identical species. Our present study is the first demonstration of reliable identification of glycopeptide-intermediate *S. aureus* by FTIR spectroscopy.

The decrease in the discrimination between epidemic MRSA and GISA/hGISA from 100% to 84.15% with 13 sporadic MRSA misclassified indicates poor specificity in the 1352–1315 cm^{-1} region. This may indicate heterogeneity of this phenotype, resulting from the acquisition of SCCmec by strains of different genetic background. In comparison, discrimination using the spectral region of 1480–1460 cm^{-1}, containing primarily absorption bands that may be assigned to CH_2 asymmetric bending vibrations of lipids and proteins,[36,37] was not affected by the inclusion of the 22 sporadic MRSA isolates. On the basis of the interpretations for MIC breakpoints and recommendations of the CDC[38] and CLSI,[39] the misclassified GISA/hGISA NRS4 has shown intermediate resistance to vancomycin and teicoplanin by BHIA-MMET and a susceptible-resistant pattern by all other screening methods (BMD, MHA-CMET, BHIA-6V and DD), except for intermediate teicoplanin resistance using MHA-CMET. The other misclassified GISA/hGISA (NRS68) has shown intermediate resistance to vancomycin and susceptibility to teicoplanin using BHIA-MMET. All the other screening methods used (BMD, MHA-CMET, BHIA-6V and DD) have indicated no resistance to either glycopeptide. The four sporadic MRSA strains (715, 864, 693 and 105) apparently misclassified by FTIR as glycopeptide intermediate using PCA, as well as the sporadic MRSA 182 misclassified by SOM, have never in fact been tested for glycopeptide susceptibility.

An explanation for the repeated misclassification of GISA/hGISA isolates NRS4 and NRS68 by PCA and KNN could not be advanced on the basis of their vancomycin and teicoplanin susceptibility patterns. However, it should be noted that the glycopeptide-intermediate resistance phenotype may be unstable and affected by subculture methodology, repeated subculture or by different growth media used prior to susceptibility testing. Uniform decreases in vancomycin and teicoplanin MICs occurred after 15 days of serial passage on non-selective medium,[40–42] a situation that provides an opportunity for reversion to occur. Reversion of the glycopeptide-intermediate resistance phenotype can occur in all types of GISA/hGISA isolates,[40,42,43] although it appears to depend on the genetic background of the bacterial strain to some extent.[40] This reversion may account for some of the difficulties in identifying them in the clinical laboratory and may explain the misidentification of isolates NRS4 and NRS68. All isolates in the present study were activated in the blood agar and cultured on Que-Bact® Universal Medium No. 2, both without glycopeptides, prior to FTIR analysis.

The identification of GISA/hGISA isolates NRS4 (HIP5836) and NRS68 should be confirmed by quantitative susceptibility and confirmatory testing using PAPs, whereas the sporadic MRSA strains 715, 864, 693, 105 and 182 should be tested for glycopeptide resistance by conventional screening methods to determine whether or not our FTIR method did in fact misclassify them.

Conclusions

On the basis of the results of this study, FTIR spectroscopy combined with the use of growth medium Que-Bact® Universal Medium No. 2 and chemometric analysis of spectral data appear to offer a promising alternative to conventional susceptibility testing methods for routine identification of GISA/hGISA and accordingly warrant further validation studies to confirm the suitability of this technique for rapid screening of these strains. In addition, further investigation of the spectral differences between MRSA and GISA/hGISA isolates observed in this study may aid in the elucidation of the mechanisms of glycopeptide resistance in MRSA.

Acknowledgements

We thank the Canadian Nosocomial Infection Surveillance Program (CNISP) for participating in this research. GISA/hGISA isolates were obtained through the Network on Antimicrobial Resistance in *S. aureus* (NARSA) programme, supported by the US National Institute for Allergy and Infectious Diseases (US National Institutes of Health, contract N01-AI-95359).

Funding

This work was funded by Quelab Laboratories Inc.

Transparency declarations

None to declare.

Supplementary data

Colour versions of Figures 1–4 are available as Supplementary data at *JAC* Online (http://jac.oxfordjournals.org/).

References

1. Hiramatsu K, Aritaka N, Hanaki H *et al.* Dissemination in Japanese hospitals of strains of *Staphylococcus aureus* heterogeneously resistant to vancomycin. *Lancet* 1997; **350**: 1670–3.

2. Smith TL, Pearson ML, Wilcox KR *et al.* Emergence of vancomycin resistance in *Staphylococcus aureus*. *N Engl J Med* 1999; **340**: 493–501.

3. Centers for Disease Control and Prevention. Vancomycin-resistant *Staphylococcus aureus*—Pennsylvania, 2002. *Morb Mortal Wkly Rep* 2002; **51**: 902.

4. Walsh TR, Howe RA. The prevalence and mechanisms of vancomycin resistance in *Staphylococcus aureus*. *Ann Rev Microbiol* 2002; **56**: 657–75.

5. Kralovic SM, Danko LH, Roselle GA. Laboratory reporting of *Staphylococcus aureus* with reduced susceptibility to vancomycin in United States department of veterans affairs facilities. *Emerg Infect Dis* 2002; **8**: 402–7.

6. Sierdzski L, Leski T, Dick J *et al*. Evolution of a vancomycin-intermediate *Staphylococcus aureus* strain *in-vivo*: multiple changes in the antibiotic resistance phenotypes of a single lineage of methicillin-resistant *S. aureus* under the impact of antibiotic administration. *J Infect Dis* 2003; **186**: 661–7.

7. Moore MR, Perdreau-Remington F, Chambers HF. Vancomycin treatment failure associated with heterogeneous vancomycin- intermediate *Staphylococcus aureus* in a patient with endocarditis and in the rabbit model of endocarditis. *Antimicrob Agents Chemother* 2003; **47**: 1262–6.

8. Tenover FC, Lancaster MV, Hill BC *et al*. Characterization of staphylococci with reduced susceptibilities to vancomycin and other glycopeptides. *J Clin Microbiol* 1998; **36**: 1020–7.

9. Walsh TR, Bolmström A, Quarnstrom A *et al*. Evaluation of current methods of detecting vancomycin resistance and hetero-resistance in *Staphylococcus aureus* and other staphylococci. *J Clin Microbiol* 2001; **39**: 2439–44.

10. Wootton M, Howe RA, Hillman R *et al*. A modified population analysis profile (PAP) method to detect hetero-resistance to vancomycin in *Staphylococcus aureus* in a UK hospital. *J Antimicrob Chemother* 2001; **47**: 399–403.

11. Mallaval F-O, Carricajo A, Delavenna F *et al*. Detection of an outbreak of methicillin-resistant *Staphylococcus aureus* with reduced susceptibility to glycopeptides in a French hospital. *Clin Microbiol Infect* 2004; **10**: 459–61.

12. Bhateja P, Purnapatrek K, Dube S *et al*. Characterisation of laboratory-generated vancomycin-intermediate resistant *Staphylococcus aureus* strains. *Int J Antimicrob Agents* 2006; **27**: 201–11.

13. Hubert SK, Mohammed JM, Fridkin SK *et al*. Glycopeptide-intermediate *Staphylococcus aureus*: evaluation of a novel screening method results of a survey of selected US hospitals. *J Clin Microbiol* 1999; **37**: 3590–3.

14. Aucken HM, Warner M, Ganner M *et al*. Twenty months of screening for glycopeptide-intermediate *Staphylococcus aureus*. *J Antimicrob Chemother* 2000; **46**: 639–40.

15. Wootton M, MacGowan AP, Walsh TR *et al*. A multi-center study evaluating the current strategies for isolating *Staphylococcus aureus* strains with reduced susceptibility to glycopeptides. *J Clin Microbiol* 2007; **45**: 329–32.

16. Sieradzki K, Tomasz A. Gradual alterations in cell wall structure and metabolism in vancomycin-resistant mutants of *Staphylococcus aureus*. *J Bacteriol* 1999; **181**: 7566–70.

17. Naumann D, Helm D, Labischinski H *et al*. The characterization of microorganisms by Fourier-transform infrared spectroscopy. In: Nelson WH, ed. *Modern Techniques for Rapid Microbiological Analysis*. New York: VCH Publishers, 1991; 43–96.

18. Kirschner C, Maquelin K, Pina P *et al*. Classification and identification of *Enterococci*: a comparative phenotypic, genotypic, and vibrational spectroscopic study. *J Clin Microbiol* 2001; **39**: 1763–70.

19. Maquelin K, Kirschner C, Choo-Smith L-P *et al*. Prospective study of the performance of vibrational spectroscopies for rapid identification of bacterial and fungal pathogens recovered from blood cultures. *J Clin Microbiol* 2003; **41**: 324–9.

20. Mariey L, Signolle JP, Amiel C *et al*. Discrimination, classification, identification of microorganisms using FTIR spectroscopy and chemometrics. *Vibr Spectrosc* 2001; **26**: 151–9.

21. Miguel Gomez MA, Bratos Perez MA, Martin Gil FJ *et al*. Identification of species of *Brucella* using Fourier transform infrared spectroscopy. *J Microbiol Methods* 2003; **55**: 121–31.

22. Winder CL, Carr E, Goodacre R *et al*. The rapid identification of *Acinetobacter* species using Fourier transform infrared spectroscopy. *J Appl Micobiol* 2004; **96**: 328–39.

23. Bouhedja W, Sockalingum GD, Pina P *et al*. ATR-FTIR spectroscopic investigation of *E. coli* transconjugants β-lactams-resistance phenotype. *FEBS Lett* 1997; **412**: 39–42.

24. Kirschner C, Ngo Thi NA, Naumann D. FT-IR spectroscopic investigations of antibiotic sensitive and resistant microorganisms. In: *Second Workshop on FT-IR Spectroscopy in Microbiology and Medical Diagnostic*. Robert Koch-Institute, Berlin, 2000.

25. Sockalingum GD, Bouhedja W, Pina P *et al*. ATR-FTIR spectroscopic investigation of imipenem susceptible and resistant *Pseudomonas aeruginosa* isogenic strains. *Biochem Biophys Res Commun* 1997; **232**: 240–6.

26. Naumann D. Infrared spectroscopy in microbiology. In: Meyers RA, ed. *Encyclopedia of Analytical Chemistry*. Chichester: John Wiley & Sons Ltd, 2000; 102–31.

27. Golub GH, van Loan CF. The singular value decomposition and unitary matrices. In: Johns Hopkins University Press, ed. *Matrix Computations*. Baltimore, MD: Johns Hopkins University Press, 1996; 70–71 and 73.

28. Jolliffe IT. *Principal Component Analysis.* Springer Series in Statistics. New York: Springer-Verlag, 1986.

29. Kohonen T. *Self-Organizing Maps.* Vol. 30 of Springer Series in Information Sciences. Berlin, Heidelberg, New York: Springer-Verlag, 1995.

30. Adams MJ. Pattern recognition II: supervised learning. In: Barnett RA, ed. *Chemometrics in Analytical Spectroscopy*. Letchworth: The Royal Society of Chemists Analytical Spectroscopy Monographs. Turpin Distribution Services Ltd, 1995; 123–42.

31. Bourne R, Himmelreich U, Sharma A *et al*. Identification of *Enterococcus*, *Streptococcus*, and *Staphylococcus* by multivariate analysis of proton magnetic resonance spectroscopic data from plate cultures. *J Clin Microbiol* 2001; **39**: 2916–23.

32. Naumann D. Some ultrastructural information on intact, living bacterial cells and related cell-wall fragments as given by FTIR. *Infrared Phys* 1984; **24**: 233–8.

33. Magee J. Whole-organism fingerprinting. In: Goodfelow M, O'Donnel AG, eds. *Handbook of New Bacterial Systematics*. New York: Harcourt Brace, 1993; 383–427.

34. Kümmerle M, Scherer S, Seiler H. Rapid and reliable identification of food-borne yeasts by Fourier-transform infrared spectroscopy. *Appl Environ Microbiol* 1998; **64**: 2207–14.

35. Diem M. *Introduction to Modern Vibrational Spectroscopy*. New York: John Wiley and Sons, 1994.

36. Alban JO, Fiamingo FG. Fourier transform infrared spectroscopy. In: Rousseau DL, ed. *Optical Techniques in Biological Research*. New York: Academic Press, 1984; 133–79.

37. Mordechai S, Salman A, Argov S *et al*. In: Mahadevan-Jansen A, Puppels GJ, eds. *Biomedical Spectroscopy: Vibrational Spectroscopy Other Novel Techniques, Proceedings of SPIE*. 2000; **3918**: 66–77.

38. Centers for Disease Control and Prevention. Vancomycin-resistant *Staphylococcus aureus*—New York, 2004. *Morb Mortal Wkly Rep* 2004; **53**: 322–3.

39. Clinical and Laboratory Standards Institute. *Performance Standards for Antimicrobial Susceptibility Testing: Sixteenth Informational Supplement M100-S16*. CLSI, Wayne, PA, USA, 2006.

40. Boyle-Vavra S, Berke SK, Lee JC *et al*. Reversion of the glycopeptide resistance phenotype in *Staphylococcus aureus* clinical isolates. *Antimicrob Agents Chemother* 2000; **44**: 272–7.

41. Vaudaux P, Francois P, Berger-Bachi B *et al*. *In vivo* emergence of subpopulations expressing teicoplanin or vancomycin resistance phenotypes in a glycopeptide-susceptible, methicillin-resistant strain of *Staphylococcus aureus*. *J Antimicrob Chemother* 2001; **47**: 163–70.

42. Hiramatsu K. Vancomycin-resistant *Staphylococcus aureus*: a new model of antibiotic resistance. *Lancet Infect Dis* 2001; **1**: 147–55.

43. Plipat N, Livni G, Bertram H *et al*. Unstable vancomycin heteroresistance is common among clinical isolates of methicillin-resistant *Staphylococcus aureus*. *J Clin Microbiol* 2005; **43**: 2494–6.